Mesure des champs de vitesse dans les champs hydrothermaux océaniques

E. Mittelstaedt[a], A. Davaille[a], P.E. van Keken[b], N. Gracias[c], J.Escartin[d]

a. *Laboratoire FAST (CNRS / UPMC / Univ.P-Sud) Bat.502, Rue du Belvedere, Campus Universitaire, 91405 ORSAY*

b. *Department of Geological Sciences, University of Michigan, Ann Arbor, Michigan 48109, USA*

c. *EIA Department, University of Girona, Ed. PIV, E17003 Girona, Spain*

c. *Institut de Physique du Globe de Paris/ CNRS / UPMC, F75005 Paris, France*

Résumé :

Nous présentons une nouvelle méthode pour déterminer les champs de vitesse dans les champs hydrothermaux présents sur les fonds sous-marins. Basée sur le "background-oriented schlieren", la méthode permet de suivre les anomalies d'indice de réfraction dues à la température ou la composition. Elle a été testée sur des panaches thermiques en laboratoire, puis lors d'une campagne sur la dorsale atlantique.

Abstract :

We present a new method to measure velocity distributions in the hydrothermal fields found on the deep seafloor. Based on the "background-oriented schlieren", the method allows to follow anomalies of refraction index due to temperature or composition. After tests in the laboratory on thermal plumes, it was used during a geophysical campaign on the atlantic mid-ocean ridge.

Mots clefs : **Champs de vitesse ; visualisation ; hydrothermalisme**

1 Introduction

Hydrothermal flows on the ocean floor are produced by the release of hotter fluids through fractures and vents. Since the discovery of hydrothermal venting along the mid-ocean ridges in the 1970s, it is thought that hydrothermal circulation through the oceanic crust is an important process to cool the newly formed crust at mid-ocean ridges. Moreover, these hydrothermal fields might well be the environment where life first developed in the primitive Earth. It is therefore important to characterize well these circulations.

Because hydrothermal fluids have circulated through the crust [3], they have chemically reacted with it, and therefore their composition is different from normal sea water. The density and refraction index of these hot fluids are therefore expected to differ from the sea water properties, due to temperature and composition differences : density heterogenieties, responsible for motions, will be associated with refraction index heterogeneities. A video camera recording the seafloor roughness through the lenses produced by these moving hot fluids will therefore show strong time-dependent background deformation. There are a number of well-established measurement techniques that take advantage of this property, including the Schlieren laboratory technique [11]. Recently, a whole family of imaging techniques including "Synthetic Schlieren" [2] and "Background-Oriented Schlieren" [6] have been developed to produce quantitative measurements of variations in fluid densities without the need for the complicated mirrors and lighting of standard Schlieren. These techniques determine the apparent shift of light rays passing through an index of refraction anomaly by cross-correlating the image of a reference background (placed behind a uniform fluid at rest) with the resulting image when the background is seen through a density anomaly. The result is a 2D field of apparent background deformation associated with density gradients in the fluid. In the case of a moving fluid, the apparent

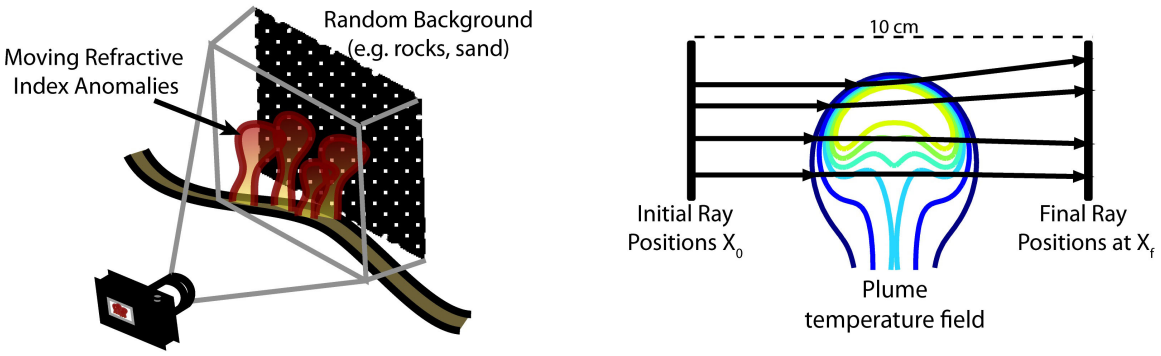

FIGURE 1 – Diffuse flow velocimetry (DFV) calculates velocities from (a) a series of images of motionless, random media (e.g., rocks or sand) obtained through moving refraction index anomalies. (b) Tests of DFV have been performed on an upwelling, laminar, axisymmetric plume created either numerically or in a laboratory tank.

deformation field is displaced along with the density gradients. These methods have been used for exemple to record and measure thermal convection from a hand [2], supersonic jets, aircraft wakes and vortices in airports [6], and waves generated on an air-water interface [8]. Here, we present a new technique, based on these methods, to characterize diffuse hydrothermal venting.

2 The Diffuse Flow Velocimetry Method (DFV)

Video sequences provide a series of images of a motionless, random medium (e.g. rocks) obtained through the lens of a moving refraction index anomaly (e.g. a hot upwelling) (Fig.1A). A DFV calculation involves two steps and three images in succession (Fig.2) ; the first determines the change in apparent deformation of subsequent background images and the second determines the movement of the apparent deformation through time to determine the fluid velocities. In the DFV first step , the deformation field is determined using Particle Image Velocimetry (PIV). A pair of consecutive images at times t_0 and t_1 are each divided into overlapping windows of L by N pixels. Here we use 8x8 to 32x32 pixels windows with an overlap of 50%. Using Fourier convolution, intensities $I^{t_0}_{l,n}$ at vertical pixel location l and horizontal pixel location n from a window at t_0 are cross-correlated with the spatially shifted window at t_1, $I^{t_1}_{l+i,n+j}$ to create a correlation matrix C_{ij} :

$$C_{ij} = \sum_{l=1}^{L} \sum_{n=1}^{N} I^{t_0}_{l,n} x I^{t_1}_{l+i,n+j} \tag{1}$$

where the indices i and j correspond to vertical and horizontal pixel shifts of the window at t_1. The location of the maximum value in the correlation matrix corresponds to the highest probability displacement of the window caused by the refraction index anomaly between t_0 and t_1. This procedure is repeated for all windows and for all subsequent image pairs. The result is an instantaneous 2D vector field of the change in the apparent background deformation due to movement of the index of refraction anomaly between each image pair. For brevity, these changes in apparent background deformation are hereafter referred to as deformation vectors or, more generally, deformation. There are several free PIV packages available that can be used to perform this first step of the process such as CIVx (http ://www.coriolis-legi.org/CIVPROJECT/main.html) and OpenPIV (http ://www.openpiv.net/). We use here mostly the LaVision DaVis software (http ://www.lavision.de/en/). But a comparison of results obtained with DaVis and with OpenPIV shows agreement within 2%.

The deformation computed by DFV is different from that obtained by Schlieren techniques where the correlation is performed in reference to a fixed, undistorted image. In DFV, the deformation vectors are computed from changes in the apparent background deformation between two subsequent images. This

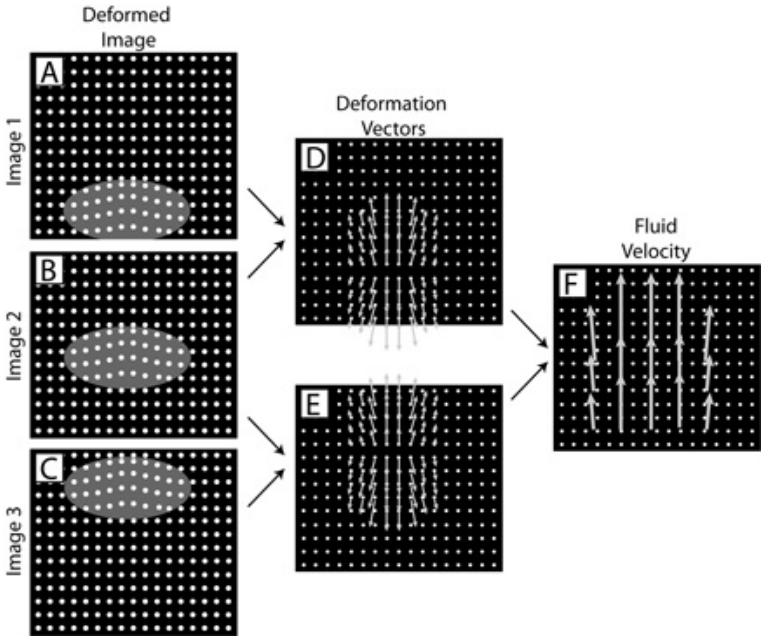

FIGURE 2 – A cartoon representation of the steps involved in DFV. (ac) Apparent deformation of a background in subsequent images is captured through the lens of a refractive index anomaly (ellipses). (d and e) The change in the apparent background deformation is calculated between these images (vectors). Finally, the location of the calculated deformations is tracked between calculations to yield (f) the fluid velocities (vectors).

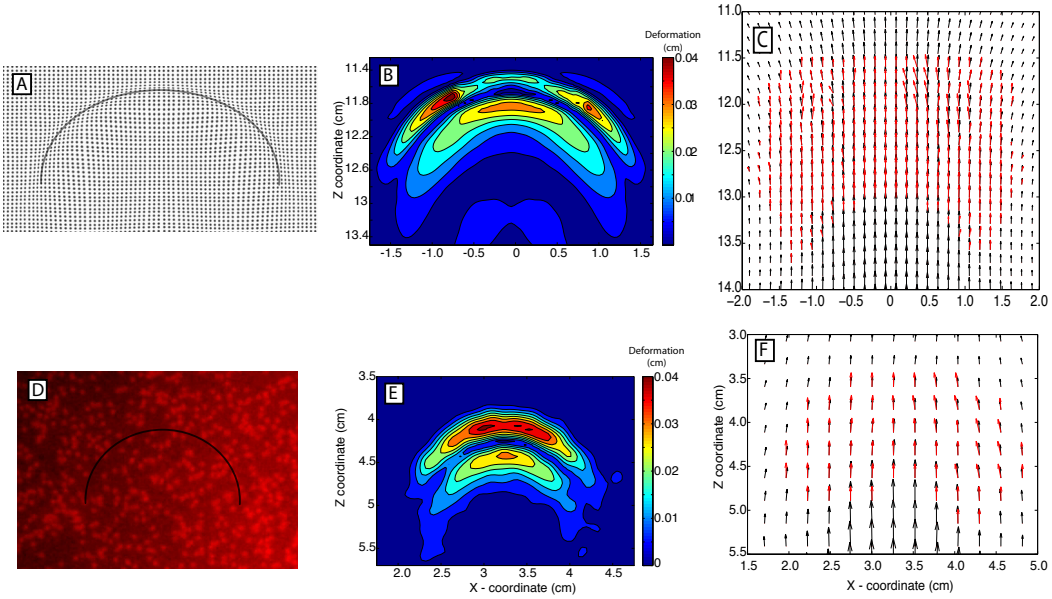

FIGURE 3 – An upwelling thermal plume acts as a refraction index anomaly causing an apparent distortion of (a) a numerically produced grid ($t = 100s$) and (d) the background of a laboratory tank ($t = 110s$). The calculated deformation magnitudes of the (b) numerical and (e) laboratory background are on the order of 0.01 cm. The DFV velocities (red arrows) are calculated by cross correlating the deformation field between successive calculations and are compared with (c) numerical velocities (black arrows) or (f) PIV velocities (black arrows) of particles imaged in the flow.

is essential in a hydrothermal environment where a reference image of the seafloor is unavailable due to continuous fluid flow. So the deformation field moves a distance d between time $t_{0.5}$ and $t_{1.5}$. If we assume that, between two calculations of the deformation field separated by a small time, the shape of the density gradients in the fluid remains nearly unchanged, d can be determined by cross-correlation of the deformation vectors. In the second step of the DFV method, two subsequent deformation vector fields at $t_{0.5}$ and $t_{1.5}$ are each divided into overlapping windows of L by N deformation vectors. We use windows of 8x8 vectors with a 50% overlap. For a single window, the correlation matrix D_{ij} is defined to be a function of both the horizontal and vertical components, X and Y, of the deformation vectors :

$$D_{ij} = \left(\frac{\sum_{l=1}^{L}\sum_{n=1}^{N}(X_{l,n}^{t_{0.5}} - X_{l+i,n+j}^{t_{1.5}})^2}{LN}\right)^{1/2} + \left(\frac{\sum_{l=1}^{L}\sum_{n=1}^{N}(Y_{l,n}^{t_{0.5}} - Y_{l+i,n+j}^{t_{1.5}})^2}{LN}\right)^{1/2} \quad (2)$$

where l and n are the local vertical and horizontal window coordinates of a deformation vector, and i and j are the vertical and horizontal window vector shifts. The location of the minimum of D_{ij} defines the highest probability displacement vector d of the window between $t_{0.5}$ and $t_{1.5}$. The precision of the location of the correlation minimum is improved from ± 0.5 times the distance between vector locations to ± 0.1 times the inter-vector distance with an analytical 3-point Gaussian fit in both coordinate directions. The use of the Gaussian fit is motivated by its rapid calculation and its low interpolation errors in PIV applications. The displacement vector d yields a velocity vector $\vec{v}(V_x, V_y)$ for the given window

$$V_x = \frac{d_x.p_x.S}{t_{1.5} - t_{0.5}}; V_y = \frac{d_y.p_y.S}{t_{1.5} - t_{0.5}} \quad (3)$$

where p_x and p_y are the horizontal and vertical number of pixels between each deformation vector, and S is the image scale. The cross-correlation is performed on all the windows to yield the instantaneous, 2D velocity field (Fig.2F). The location of the correlation minimum in Equation (2) gives the highest probability displacement of the deformation field in the window, but outliers can occur due to poor image quality, little or no fluid movement, and/or undetectable deformation (due to very small, very large, or non-existent density variations). Three methods are used to limit false correlations. First, the velocity is considered valid only if the curvature in the immediate neighborhood of the correlation minimum is greater than an empirically determined critical value of 10^{-3} to 10^{-4}. Second, a correlation minimum is considered invalid if it falls on the boundary of the correlation matrix. If a correlation minimum does not have a sufficient curvature or falls on the edge of the correlation matrix, it is assumed to be erroneous and the velocity in that location is set to 0. Finally, the calculated velocities are smoothed by a 3x3 median filter. Although this does eliminate some accurate velocities, the combination of these three methods effectively reduces the number of highly inaccurate velocities (Fig.3). The above methods for eliminating false correlations produce similar results to methods using a local roughness criteria [1]. Two sets of Matlab code are provided to facilitate the above DFV calculations in Mittelstaedt et al [7].

3 Laboratory and Numerical Tests

To evaluate the domain of applicability and accuracy of DFV, we study the simple case of a single hot buoyant plume, generated from a small circular heat source [4]. Two different, complementary, types of experiments have been performed : laboratory experiments used sugar syrup, a fluid with strongly temperature-dependent viscosity, and numerical simulations based upon a similar laboratory set-up were run with a constant viscosity fluid (silicone oil). Silicone oil and sugar syrup presents two different temperature dependence of the refraction index. The temperature gradient between the plume and the ambient fluid produces refraction index gradients that distort images of a random (laboratory) or regular (numerical) dot pattern located behind the plume (Fig.3). In the laboratory, images are captured using a red-filtered light source and camera. We use ray-tracing to construct synthetic images from the numerical results. Images of the distorted background are used to calculate fluid velocities

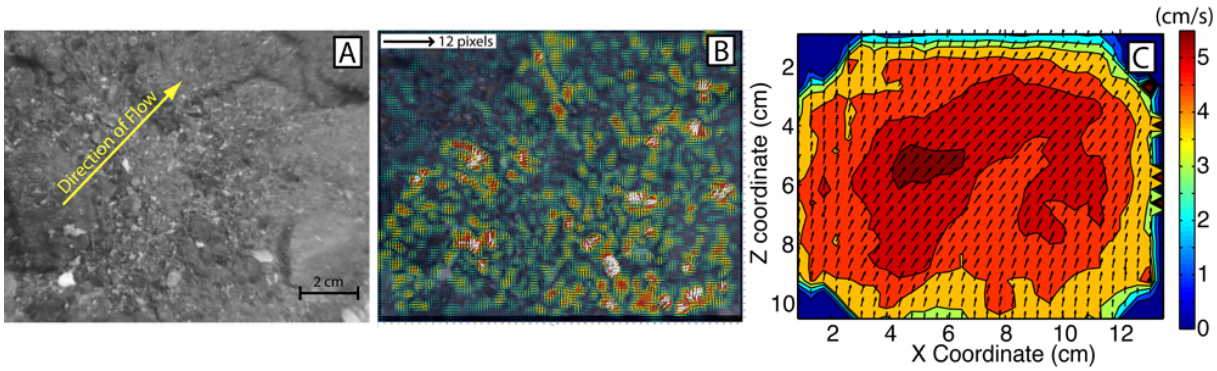

FIGURE 4 – (a) A 25 s video sequence of the seafloor, seen through the lens of moving refractive index anomalies associated with $10-15$°C diffuse effluent, is used to calculate (b) the apparent background deformation between every fifth image (hotter colors for larger magnitudes). (c) The time averaged velocities reach a maximum of 5 cm/s. The video sequence was taken in September 2009 during the Bathyluck expedition to the Lucky Strike hydrothermal field along the Mid Atlantic Ridge.

with DFV. Where the flow is time-dependent, the results compare well with known plume velocities (laboratory PIV velocities and numerical model velocities) with average RMS errors $5-7\%$. The main limitation of the method is the crossing of light rays, which may partially blurr background images and add noise to deformation calculations [8]. Our tests show that ray crossing distance is a strongly non-linear function of the vertical temperature gradient with distances between 3.3 cm and 40.3 cm for vertical thermal gradients between 4.51°C/cm and 198.6°C/cm. The crossover distances for similar thermal gradients in seawater are likely to be larger because the temperature dependence of the index of refraction is approximately one third that of our fluids.

4 Diffuse Flow from a Fracture at the Tour Eiffel Vent Site, Lucky Strike Hydrothermal Field

During the recent Bathyluck09 expedition to the Lucky Strike hydrothermal field (September, 2009) aboard the French research vessel "Pourquoi Pas ?" (IFREMER), a video survey of diffuse flow was performed along a series of fractures surrounding the Tour Eiffel vent site. Fig.4 presents an example of buoyantly-rising diffuse flow from one such fracture in a 25 second video sequence captured by the main camera on the ROV Victor 6000. The flow temperature of $10-15$°C is found by placing the ROV's onboard temperature probe in the diffuse upwelling. The probe is also used as an image scale. The camera is focused on the sandy background and the image frame is placed just above the fracture opening with a downward camera angle of 38 degrees from horizontal. To provide a stable imaging platform, the ROV is placed directly onto the seafloor near the fracture of interest. Despite this precaution, variations in the bottom current move the ROV and cause constant camera movement. The camera system records 50 frame-per-second interlaced video at a resolution of 720x540 (0.027 cm/pix). To prepare the video images for DFV calculations, the sequence is de-interlaced and the camera motion is removed by a robust feature matching algorithm [5]. Apparent background deformations are calculated between every 5th image (i.e. $\Delta t = 0.1s$) with square image windows 8 pixels to a side. The correlation of the deformation pattern is calculated between each deformation field on square windows of 8 deformation vectors to a side (Fig.4b). At the location of each calculated velocity vector, a time-average (through all 25 seconds of video) is calculated including all velocities within ± 1 of the RMS velocity at that vector location (Fig.4c).

Deformation patterns due to plume-like structures in the flow have a double-horseshoe shape with oppositely oriented distortions (Fig.4b, central-left part of image) similar to that seen in our experimental tests (Fig.3). The time-averaged DFV velocities are up to 5 cm/s in a direction up and to the right in the frame of the image. This is in good agreement with previous estimates of diffuse flow

rates from fractures, such as at the East-Pacific rise (diffuse flow velocities of 3-5 cm/s for a fluid temperature of 10°C [9]) and at the Endeavour segment of the Juan de Fuca Ridge (velocities of $7-15$ cm/s for fluids of 7°C to 13°C [10]). The fracture-based measurements are approximately an order of magnitude greater than the velocities from biological mats ($0.1-1$ cm/s, [9]). These results show that DFV can successfully measure the time-averaged 2D velocity field of diffuse effluent using only standard ROV video.

5 Conclusions

Diffuse Flow Velocimetry (DFV) is introduced as a new, non-invasive, optical technique for measuring the velocity of diffuse hydrothermal flow. The technique uses images of a motionless, random medium (e.g. rocks) obtained through the lens of a moving refraction index anomaly (e.g. a hot upwelling). The method works in two stages. First, the changes in apparent background deformation are calculated using Particle Image Velocimetry (PIV). The deformation vectors are determined by a cross-correlation of pixel intensities across consecutive images. Second, the 2D velocity field is calculated by cross-correlating the deformation vectors between consecutive PIV calculations. The domain of applicability and accuracy of the method are determined with laboratory and numerical experiments of laminar, axisymmetric plumes in fluids with both constant and temperature-dependent viscosity. Results show that average RMS errors are $5-7\%$, and that the DFV velocities are most accurate in regions of time-dependent pervasive apparent background deformation which is commonly encountered in regions of diffuse hydrothermal flow. The method is applied to a 25-second video sequence of diffuse flow from a small fracture captured during the Bathyluck'09 cruise to the Lucky Strike hydrothermal field. The velocities of the 10°C-15°C effluent reach 5 cm/s, in strong agreement with previous measurements of diffuse flow. DFV is found to be most accurate for approximately 2D flows where background objects have a small spatial scale, such as sand or gravel.

Références

[1] Crone, T. J., W. S. D. Wilcock, and R. E. McDuff 2010 Flow rate perturbations in a black smoker hydrothermal vent in response to a mid ocean ridge earthquake swarm *Geochem. Geophys. Geosyst.* **11** Q03012, doi :10.1029/ 2009GC002926.

[2] Dalziel, S. B., G. O. Hughes, and B. R. Sutherland 2000 Whole ?field density measurements by synthetic schlieren *Exp. Fluids* **28** 322335, doi :10.1007/s003480050391.

[3] German, C., and K. L. Von Damm 2003 Hydrothermal processes *in Treatise on Geochemistry, vol. 6, The Oceans and Marine Geochemistry, (ed. H. Elderfield)* pp. 181222, Elsevier, Amsterdam.

[4] A.Davaille, A. Limare, F. Touitou, I. Kumagai, J. Vatteville 2010 Anatomy of a laminar starting plume at high Prandtl number *Exp. Fluids* **50** 285-300, doi 10.1007/s00348-010-0924.

[5] Gracias, N 2003 Mosaic based visual navigation for autonomous underwater vehicles *Ph.D. thesis, Inst. Super. Tec., Lisbon.*

[6] Meier, G. E. A. 2002 Computerized background-oriented schlieren *Exp. Fluids* **33** 181187.

[7] Mittelstaedt E., A. Davaille, P. van Keken, N. Gracias, J. Escartin 2010 A non invasive method for measuring the velocity of diffuse hydrothermal flow by tracking moving refractive index anomalies *Geochem. Geophys. Geosyst* **11** Q10005, doi :10.1029/2010GC003227.

[8] Moisy F., M. Rabaud, K. Salsac 2009 A Synthetic Schlieren method for the measurement of the topography of a liquid interface *Exp. in Fluids* **46** (6), 1021-1036.

[9] Ramondenc, P., L. N. Germanovich, K. L. Von Damm, and R. P. Lowell 2006 The first measurements of hydrothermal heat output at 9°50'N, East Pacific Rise *Earth Planet. Sci. Lett.* **245** 487497, doi :10.1016/j.epsl.2006.03.023.

[10] Schultz, A., J. R. Delaney, and R. E. McDuff 1992 On the partitioning of heat flux between diffuse and point source seafloor venting *J. Geophys. Res.* **97(B9)** 12,29912,314.

[11] Topler, A 1866 Uber die methode der schlierenbeobachtung als mikroskopisches hilfsmittel, nebst bemerkungen zur theorie der schiefen beleuchtung *Ann. Phys* **203** 556580, doi :10.1002/andp.18662030405.